Anisotropy of magnetic field fluctuations in an average interplanetary magnetic cloud at 1 AU

T. W. Narock[1,2] and R. P. Lepping[3]

Received 25 July 2006; revised 2 November 2006; accepted 30 January 2007; published 8 June 2007.

[1] A subset of magnetic clouds (MCs) identified over 8.6 years of the WIND mission are examined for a pattern of anisotropic magnetic field fluctuations within their extent at 1 AU. This subset ($N = 42$) consists of MCs taken from a comprehensive survey of WIND Magnetic Field Investigation data. Root mean square deviations of the axial field ($\mathrm{RMS_A}$) and the perpendicular field ($\mathrm{RMS}_\perp$; i.e., that lying in the cross-sectional plane of the MC), rendered in a magnetic cloud coordinate system, are computed on three timescales, 8, 30, and 60 min, and a fluctuation anisotropy quantity [$A(t) = \langle \mathrm{RMS_A} \rangle / \langle \mathrm{RMS}_\perp \rangle - 1$] is calculated for each timescale. The 42 MCs are separated by relative closest approach (Y_0/R_0) into two distinct regions [$|Y_0/R_0| < 0.33$ (inner) and $0.33 < |Y_0/R_0| < 0.66$ (middle)], where R_0 is a model-estimated MC radius and Y_0 is a model-estimated magnitude of the closest-approach vector, and superimposed within each region. We show a clear and distinct magnetic field fluctuation anisotropy profile within each region. Additionally, this profile closely resembles that of the pitch angle of the field implying that the field fluctuations tend to be predominately perpendicular to the field itself. Thus transverse fluctuations are most common in MCs in the range $(1.4–10.4) \times 10^{-4}$ Hz.

Citation: Narock, T. W., and R. P. Lepping (2007), Anisotropy of magnetic field fluctuations in an average interplanetary magnetic cloud at 1 AU, *J. Geophys. Res.*, *112*, A06108, doi:10.1029/2006JA011987.

1. Introduction

[2] A magnetic cloud (MC) is defined empirically in terms of in situ spacecraft measurements of magnetic fields and thermal plasma in the interplanetary medium. That is, a MC is a transient region observed in the solar wind having (1) enhanced magnetic field strength, (2) a smooth change in field direction as observed by a spacecraft passing through the MC, and (3) low proton temperature (and low proton plasma beta) compared to the ambient solar wind properties [*Burlaga et al.*, 1981; *Burlaga*, 1988, 1995]. Typically, MCs have diameters ranging from 0.06 to 0.5 AU when observed at 1 AU with an average of about 0.25 AU. Proton plasma beta is typically around 0.12 and in some clouds has been observed as low as 0.01. This can be compared to an ambient solar wind proton plasma beta which has a typical value of about 1 or greater. MCs are also known to evolve [e.g., *Osherovich et al.*, 1993; *Bothmer and Schwenn*, 1998; *Berdichevsky et al.*, 2003], and consistent with their large size, their durations are long, usually between about 10 and 48 hours at 1 AU, but a small percentage of events have durations as short as 5 hours. See the work of *Lepping et al.* [2003] for an average MC profile at 1 AU in terms of fundamental scalar quantities based on WIND observations over several early years of the mission, and the work of *Lepping et al.* [2006] for a quantitative summary of the characteristics of WIND MCs for the first 8.6 years of the mission.

[3] A MC is usually either coincident with, or at least part of, an interplanetary coronal mass ejection, although the terms are not usually used synonymously. For example, *Gopalswamy et al.* [1998] show MCs to be often related to coronal mass ejections (CMEs) appearing to be the "core" region within a CME where the magnetic field is enhanced (also see *Gosling* [1990, 1997]). *Bothmer and Schwenn* [1994] argue that CMEs associated with erupting prominences are the sources of interplanetary magnetic clouds. Additionally, *Webb et al.* [2000] linked the May 1997 CME with WIND observations of a MC. In the solar wind, a MC is usually observed to be a special kind of large magnetic flux rope [*Marubashi*, 1986, 1997; *Burlaga et al.*, 1990; *Lepping et al.*, 1990], but MCs are not always easily nor accurately modeled as such. For a discussion of various kinds of magnetic flux ropes and their models, see the study by *Priest* [1990].

[4] Observations show that there are obvious magnetic field deviations from any ideally envisioned flux rope in most MCs, and these may be wave-like or more random in nature. In this work, we will refer to all such deviations simply as fluctuations in the field. The principal intent here is to ascertain if the fluctuations in the magnetic field within an "average" MC at 1 AU are mainly isotropic or anisotropic, and, if the latter, to find how this anisotropy varies in

[1]Goddard Earth and Science Technology Center, University of Maryland, Baltimore County, Baltimore, Maryland, USA.
[2]Heliospheric Physics Laboratory, GSFC/NASA, Greenbelt, Maryland, USA.
[3]Space Weather Laboratory, GSFC/NASA, Greenbelt, Maryland, USA.

Copyright 2007 by the American Geophysical Union.
0148-0227/07/2006JA011987

terms of percent duration through the "average" MC. By our terminology, isotropic means that the fluctuation level aligned with the MC's axis is equal to that in the cross-sectional plane.

2. Data Set

[5] *Lepping et al.* [2006] performed a comprehensive study of MCs over 8 years of the WIND mission and identified 82 MCs. Subsequently, model parameters were found for all 82 MCs using a force free flux rope model [*Lepping et al.*, 1990] based on Bessel functions. This study focuses on the WIND Magnetic Field Investigation (MFI) data [*Lepping et al.*, 1995] and a subset of those 82 MCs. *Lepping et al.* [2006] defined a quantitative estimate of a model fit quality, and we begin by excluding the poorest quality MC events from that study. In order to convert from geocentric solar ecliptic (GSE) coordinates (the initial representation of the data) to the cloud coordinate system used in this study, it is essential to know the cloud axial latitude and longitude. These angles are determined from the model fit, along with other quantities used in estimating quality. Furthermore, MCs less than 10 hours in duration are excluded. As mentioned previously, a typical MC ranges in duration from 10 to 48 hours at 1 AU. A few short-duration MCs were found but not included in this study as a means to better estimate the profile of an "average" MC. Finally, the relative closest approach is calculated and used as a means of exclusion. Relative closest approach is given by CA = $|Y_0/R_0|$, where R_0 is the model-estimated radius and Y_0 is the model-estimated magnitude of the closest-approach vector. Those events having a closest approach within the inner region of the cloud (CA < 0.33) and the middle region (0.33 < CA < 0.66) were kept. This results in a subset of 42 MCs.

3. Analysis

[6] The MCs are first split into the two aforementioned regions based on closest-approach values. The front and rear boundaries of the MCs are found by visual inspection of the data. Initially, lower-resolution data (15- to 30-min averages) were used in the model fitting. This resolution is ideal for studying the global properties of these long-duration MCs; however, for this study, it is important to know the boundaries more precisely. Thus 1-min data were visually examined in the vicinity of the model-estimated boundaries to better identify the front and rear boundaries of the MCs. Next, the GSE MC data are transformed into a cloud coordinate system (denoted by the CL subscript). In this coordinate system, the x_{CL} component is along the axis of the MC (and positive along **B**), and the y_{CL} and z_{CL} components are parallel to the MC's cross section, where y_{CL} is the magnitude of the closest-approach vector. The transformation matrix from GSE to cloud coordinates is given by:

$$M = \begin{bmatrix} \cos\theta_{\mathrm{A}}\cos\phi_{\mathrm{A}} & \cos\theta_{\mathrm{A}}\sin\phi_{\mathrm{A}} & \sin\theta_{\mathrm{A}} \\ -\sin\phi_{\mathrm{A}}\cos\psi - \sin\theta_{\mathrm{A}}\cos\phi_{\mathrm{A}}\sin\psi & \cos\phi_{\mathrm{A}}\cos\psi - \sin\theta_{\mathrm{A}}\sin\phi_{\mathrm{A}}\sin\psi & \cos\theta_{\mathrm{A}}\sin\psi \\ \sin\phi_{\mathrm{A}}\sin\psi - \sin\theta_{\mathrm{A}}\cos\phi_{\mathrm{A}}\cos\psi & -\cos\phi_{\mathrm{A}}\sin\psi - \sin\theta_{\mathrm{A}}\sin\phi_{\mathrm{A}}\cos\psi & \cos\theta_{\mathrm{A}}\cos\psi \end{bmatrix} \quad (1)$$

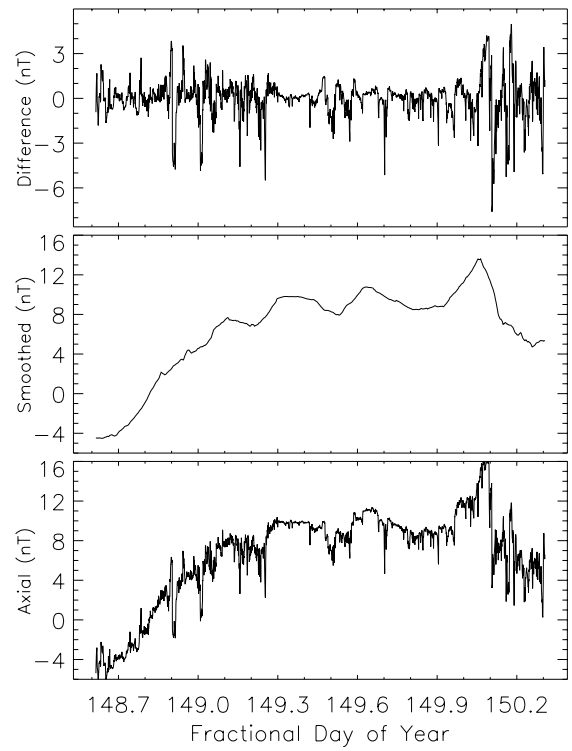

Figure 1. May 27–29 1996 MC. Plotted in the bottom panel is the 1-min averaged axial component of the MC. Middle panel shows the smoothed data using a 121-min window, and top panel is the difference field on a 1-min basis.

where ϕ_{A} and θ_{A} are the MC axis longitude and latitude angles, respectively, determined from the model fit. The angle ψ is related to ϕ_{A} and θ_{A} by:

$$\psi = \tan^{-1}\left(-\tan\phi_{\mathrm{A}}/\sin\theta_{\mathrm{A}}\right) \quad (2)$$

For a complete description of the transformation along with an illustration and derivation, see http://lepmfi.gsfc.nasa.gov/mfi/ecliptic.html. The three cloud coordinate components are then used to compute B_{A} (axial field, $B_{\mathrm{A}} = B_{xcl}$) and $B_{\perp}$ (perpendicular field lying in the cross-sectional plane of the cloud, $B_{\perp} = \sqrt{(B_{ycl}^2 + B_{zcl}^2)}$.

[7] Since, by definition, the MC's magnetic field rotates as the MC passes the observer, it will contribute to any calculation of a root mean square (RMS) deviation of the field. The MC's field is therefore considered an undesirable background field to be eliminated before RMS estimations. This is done by detrending the data before the fluctuation analysis begins. The trend field is subtracted from the original field to provide a difference field to which the RMS analysis is applied. We choose a simple box car running average for obtaining a low-frequency estimation of the background trend field. Various box car intervals were tested to find an optimum one to be used for all further

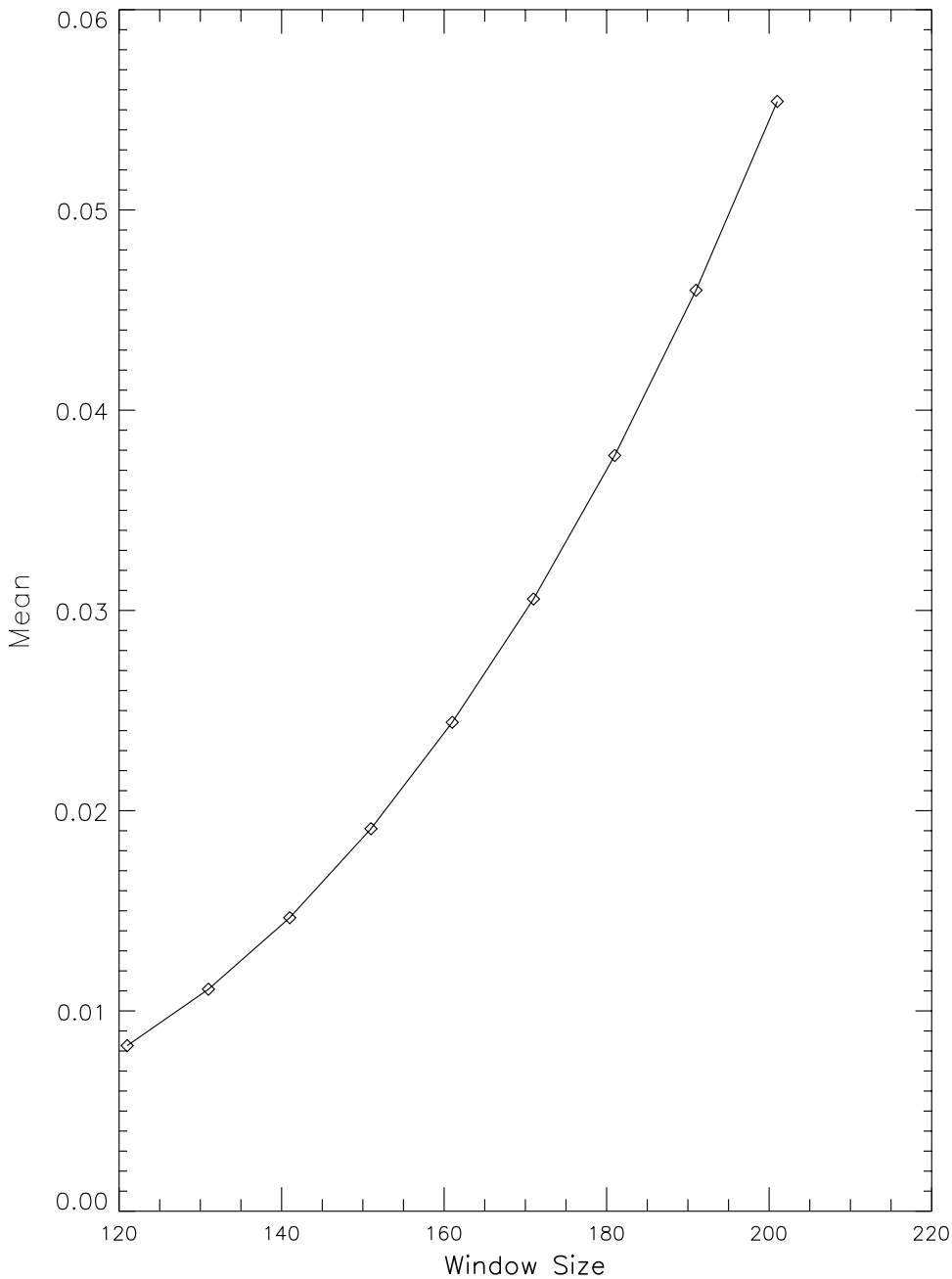

Figure 2. Mean of $\langle \Delta B_A \rangle^2$ for the inner set as a function of box car window size.

analysis. Our philosophy in this regard is to obtain an interval that is intermediate in length, i.e., not too short (whereby the resulting estimate of the background field is subject to the whim of the actual fluctuations and waves in the data) and not too long (whereby the estimated background field will not track fast enough allowing some low frequencies of the MC to leak into the resulting difference fields). We form box car lengths with an odd number of 1-min averages and therefore consider an 11-min length too short and 601-min length (a half-duration for a typical 20 hour MC [*Lepping and Berdichevsky*, 2000]) too long. Since the average axial field of the MC, $\langle B_A \rangle$, is always positive for all well-determined cases (and generally so for even not so well determined cases), this fact can be utilized in helping to determine a range of acceptable box car lengths. For various lengths, we generate $\langle \Delta B_A \rangle$, which is the average of the difference between the observations and the detrended data. This quantity should ideally be zero, if the box car's length is long enough to provide good statistics and no significant flux rope field is leaking in. Since we will be considering RMSs based on intervals as long as 60 min, we start by examining box cars about twice this, i.e., of 121 min. This length is applied to all the clouds in the inner set ($N = 24$) yielding an array of $\langle \Delta B_A \rangle$ values. These values are then squared and the mean is determined. Successive lengths are taken, and the optimum box car

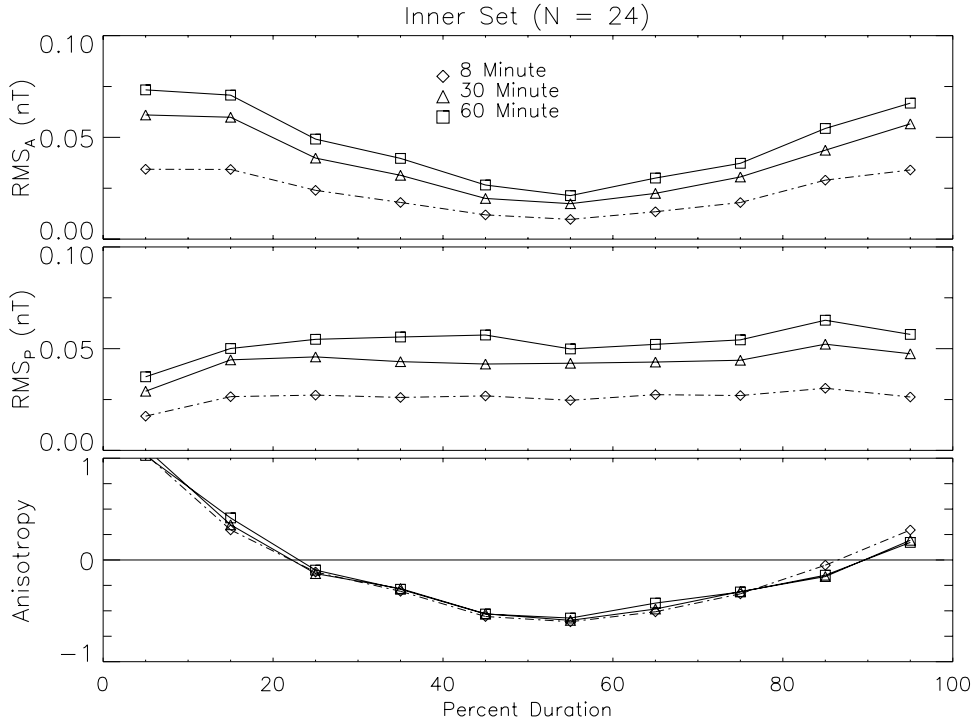

Figure 3. Plotted in the bottom panel is the anisotropy for the inner set. Middle panel shows the perpendicular RMS, and top panel shows the axial RMS. All quantities are displayed as a function of percent duration through an "average" MC.

length is chosen to be the length with the minimum mean. Figure 1 shows the axial component of a typical MC, both in the original data and the box car smoothed data, along with the difference field. Additionally, Figure 2 shows the means of $\langle \Delta B_A \rangle^2$ as a function of box car length, for lengths of 121 min and greater. As can clearly be seen, the mean of $\langle \Delta B_A \rangle^2$ increases with box car length, and the optimal choice is 121 min.

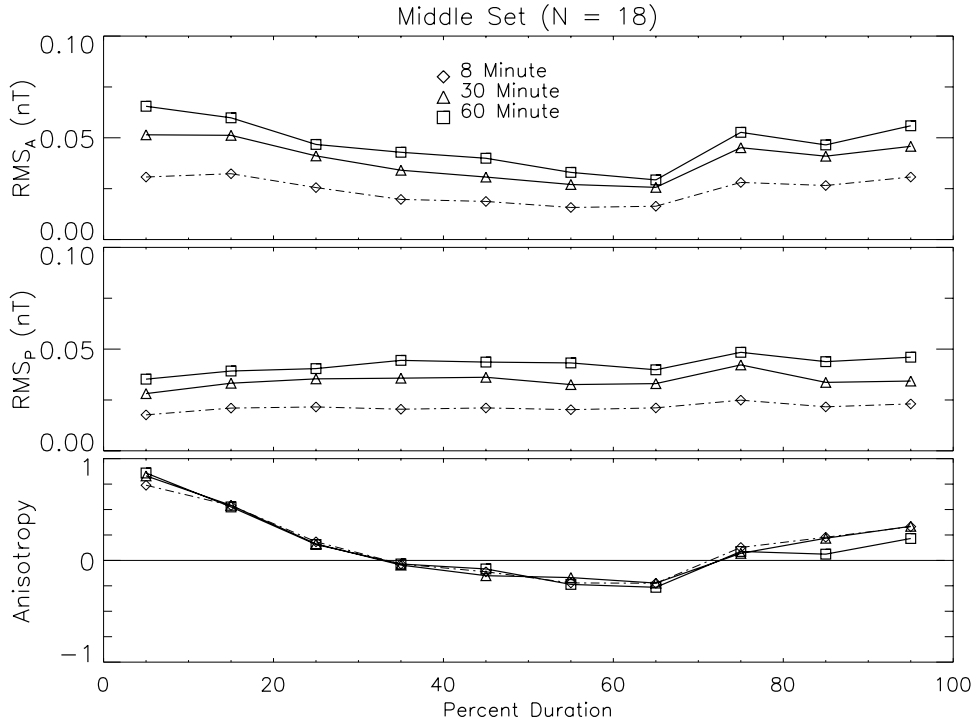

Figure 4. Plotted in the bottom panel is the anisotropy for the middle set. Middle panel shows the perpendicular RMS, and top panel shows the axial RMS. All quantities are displayed as a function of percent duration through an "average" MC.

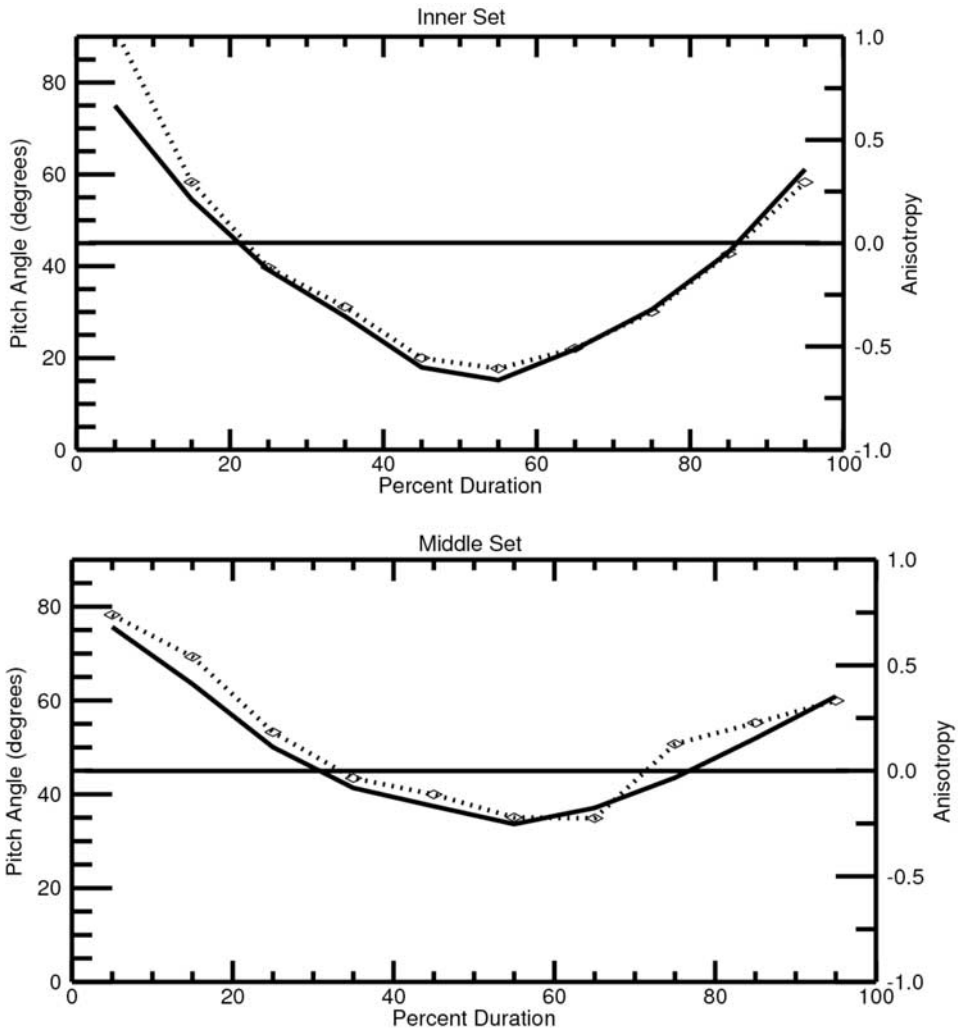

Figure 5. Pitch angle of an "average" MC for the inner and middle sets (solid line). The anisotropy for the 8-min set for each region is shown plotted with the dashed line.

[8] RMS deviations of the difference fields, ΔB_A and $\Delta B_\perp$, are calculated across the clouds over time intervals 8, 30, and 60 min using the optimal box car window size of 121 min to detrend the data, where RMS is given by:

$$\mathrm{RMS}(t) = \sqrt{(1/N)\sum_{i=1}^{N}(B_i - \langle B\rangle)^2} \tag{3}$$

where B is either B_A or $B_\perp$.

[9] To compare the results and examine the profile of an "average" MC at 1 AU, we place the inner and middle sets, respectively, on a common temporal basis, that of percent duration, and calculate $\langle \mathrm{RMS_A}\rangle$ and $\langle \mathrm{RMS}_\perp\rangle$ for each 10% duration. We further define the quantity

$$A(t) = \langle \mathrm{RMS_A}(t)\rangle / \langle \mathrm{RMS}_\perp(t)\rangle - 1, \tag{4}$$

an "anisotropy," such that for $A < 0.0$, perpendicular fluctuations dominate, and for $A > 0.0$, axial fluctuations dominate. $A = 0.0$ represents the isotropic case. Henceforth, it is understood that all quantities depend on time, so it will be dropped explicitly in the following equations.

4. Results

[10] Figures 3 and 4 show $\langle \mathrm{RMS_A}\rangle$, $\langle \mathrm{RMS}_\perp\rangle$, and anisotropy for the inner and middle regions, respectively. In both regions, and for $\langle \mathrm{RMS_A}\rangle$ and $\langle \mathrm{RMS}_\perp\rangle$, the fluctuation amplitudes are highest for the 60-min set and lowest for the 8-min set everywhere, but A is similar for all three sets. Thus the anisotropy profile is independent of RMS window size. Furthermore, the profiles are roughly symmetric around the 50% point (the expected closest-approach point) and reminiscent of the field rotation in the flux rope model representation used to fit the data.

[11] The pitch angle (θ_p) of the field at any point in a MC is given by

$$\theta_p = \tan^{-1}(|B_\perp|/B_A), \tag{5}$$

where pitch angle is defined as the angle between the field direction and the MC axis. The Bessel function representa-

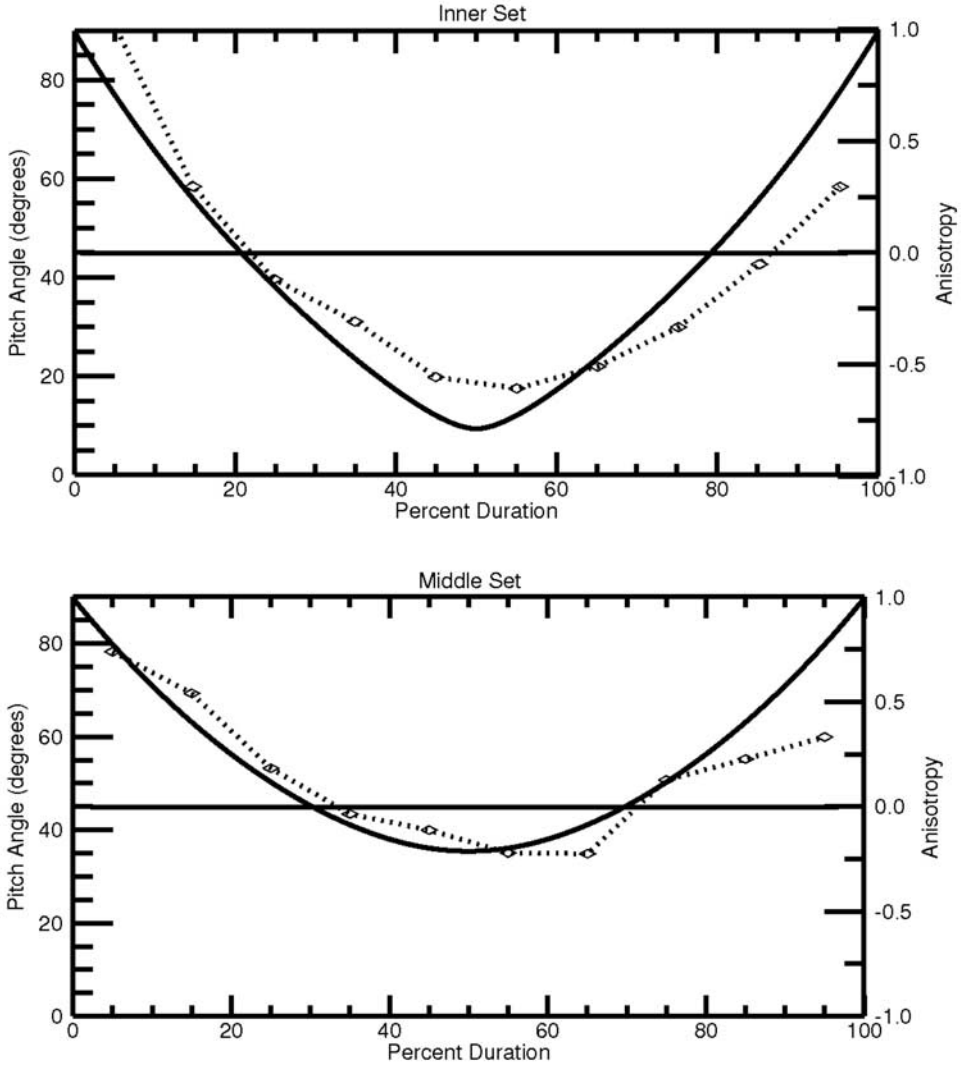

Figure 6. Modeled pitch angle using a force free Bessel function representation of a magnetic cloud (solid line). The 8-min anisotropy profile is shown as well, plotted with the dashed line.

tion [e.g., see *Goldstein*, 1983; *Lundquist*, 1950] for the pitch angle (θ_M) of a force free flux rope is given by

$$\theta_M = \tan^{-1}\left(|J_1(\alpha r)|/J_0(\alpha r)\right) \quad (6)$$

where in this case

$$B_A = B_O J_0(\alpha r) \text{ and } B_\perp = B_T = B_O H J_1(\alpha r). \quad (7)$$

B_O is the model-estimated magnitude of the field on the axis, H is the handedness of the field, $J_0(\alpha r)$ and $J_1(\alpha r)$ are the zeroth and first-order Bessel functions, r is the radial distance from the rope's axis, and α is chosen to be $2.4/R_O$ [so the MC's boundary, at R_O, is approximately where $J_0(\alpha r)$ has its first zero]. Note that $B_\perp = B_T$ because the radial component is exactly zero in this model.

[12] The observed pitch angle θ_p is computed using the average measured axial and perpendicular fields. Figure 5 shows θ_p versus percent duration for both the inner and middle regions. Plotted with θ_p is the 8-min anisotropy (dashed curve).

[13] First, we notice that A is positive for all $\theta_p > 45°$ and negative for all $\theta_p < 45°$ in both the inner and middle regions. This indicates that perpendicular fluctuations dominate where the field is axial (closer to the axis), and axial fluctuations dominate when the field is perpendicular to the axis (closer to the boundary). In other words, the dominating fluctuations are generally transverse. When A is compared to the modeled pitch angle θ_M in Figure 6, we see good agreement in the front and midsection of the MC. However, the rear of the MC deviates slightly from the model profile.

[14] Observations of magnetic field fluctuations perpendicular to the mean magnetic field in the solar wind were first reported by *Belcher and Davis* [1971]. Subsequent work [*Matthaeus et al.*, 1990; *Bieber et al.*, 1996; *Leamon et al.* 1998] advanced the theory of solar wind turbulence and perpendicular field fluctuations. In terms of MCs, *Leamon et al.* [1998] first reported seeing transverse fluctuations within the January 1997 MC. Their analysis of a MC embedded within an interplanetary coronal mass ejection showed that transverse fluctuations dominate

within a MC and are more prevalent than what is seen in the ambient solar wind. This was attributed to the low plasma beta seen within MCs and its effects on reduced magnetohydrodynamic (MHD) equations [*Zank and Matthaeus*, 1992].

[15] Here we have extended the work of *Leamon et al.* [1998] to show that the "average" MC follows this profile. Our statistical study expands upon their single case in order to understand the general profile of magnetic field fluctuations within MCs and to better understand the global properties of MCs at 1 AU. The examination of the anisotropy of 42 MCs has shown that the "average" MC very closely approximates the observed pitch angle profile, and it also approximates to a good extent the Bessel function representation of the pitch angle.

[16] A slight deviation from the Bessel function representation occurs at the rear of the "average" MC, from approximately 75% to 100% duration. The Bessel function formulation for MC parameter fitting has shown success in the past [see *Lepping et al.*, 1990] and is the formulation used to determine the cloud longitude and latitude angles in this study. It is also the basis for the cloud coordinate system. For completeness, we have also compared the anisotropy profile to the model-calculated pitch angle. Inspection of Figure 6 indicates generally good agreement of the anisotropy profile with the model pitch angle, except for the slight deviation at the rear of the "average" MC. While the fluctuations in the rear of the MC are axial, they are not of the magnitude expected by the model pitch angle. This deviation is surprising and could arise from a number of sources. One of which may be a non-well-defined rear boundary and interactions with the trailing solar wind. It opens avenues for future model development and is a topic of future study. Although there is a slight discrepancy between model and data, there is clear indication that transverse fluctuations dominate throughout.

5. Summary and Conclusions

[17] Forty-two WIND MCs, representing a subset of the 82 MCs identified over the first 8.6 years of the mission, are tested for the possibility of a pattern of anisotropic magnetic field fluctuations within their extent at 1 AU. RMS deviations of the axial and perpendicular difference fields, rendered in a magnetic cloud coordinate system, are examined separately and relatively in terms of the quantity $A = \langle \mathrm{RMS_A} \rangle / \langle \mathrm{RMS_\perp} \rangle - 1$, called anisotropy, where $\langle \mathrm{RMS_A} \rangle$ and $\langle \mathrm{RMS_\perp} \rangle$ are the axial and perpendicular RMSs, respectively. These quantities are computed and analyzed separately on three timescales, 8, 30, and 60 min, and for two different relative closest approach (Y_0/R_0) regions of $|Y_0/R_0| < 0.33$ (the inner region) and $0.33 < |Y_0/R_0| < 0.66$ (the middle region), where R_0 is the estimated radius of the magnetic cloud and $|Y_0|$ is the magnitude of the spacecraft's closest-approach vector. The 42 MCs are then superimposed according to these discriminators and plotted against percent duration. When the inner region is considered (where $N = 24$), a very clear pattern emerges showing that, for all three timescales, A is above 0 in the early portions of the structure, below 0 in the center, and above 0 in the latter portions (see Figure 3). For the middle region (where $N = 18$), we see that A has a similar profile, again for all three timescales, but is generally shifted positively such that the central minimum value is distinctly greater than it was for the inner region (see Figure 4). We show that this profile of A versus percent duration through the MC very closely resembles that of the observed pitch angle (θ_p) of the field. In particular, positive and negative values of A are fairly well separated by a θ_p of 45°; that is, A is positive for approximately all $\theta_p > 45°$ and negative for approximately all $\theta_p < 45°$. This implies that the fluctuations in the field (as measured by relative RMS) tend to be predominantly perpendicular to the field itself, everywhere. Hence transverse fluctuations are most common in MCs at 1 AU in the frequency range $(1.4–10.4) \times 10^{-4}$ Hz.

[18] When A is compared to the Bessel function representation of a force free flux rope, i.e., using equations (6) and (7), the rear of the cloud does not strictly follow the expected θ_M pattern. This fact could be attributed, at least partially, to a non-well-defined rear boundary and interactions of the MC with the trailing solar wind. The Bessel function representation has shown success in the past, and these deviations provide insight into expanding the model and improving its future usage.

[19] **Acknowledgments.** The authors would like to thank Adam Szabo, data manager for the WIND MFI instrument, for providing access to the highest quality processed MFI data.

[20] Zuyin Pu thanks Volker Bothmer and Dastgeer Shaikh for their assistance in evaluating this paper.

References

Belcher, J. W., and L. Davis (1971), Large-amplitude Alfven waves in the interplanetary medium, *J. Geophys. Res.*, *76*(16), 3534–3563.

Berdichevsky, D. B., R. P. Lepping, and C. J. Farrugia (2003), Geometric consideration of the evolution of magnetic flux ropes, *Phys. Rev.*, E 67, 036405, 1–8.

Bieber, J. W., W. Wanner, and W. H. Matthaeus (1996), Dominant two-dimensional solar wind turbulence with implications for cosmic ray transport, *J. Geophys. Res.*, *101*, 2511–2522.

Bothmer, V., and R. Schwenn (1994), Eruptive prominences as sources of magnetic clouds in the solar wind, Proceedings of the II Soho Workshop at Elba, Italy, 1993, *Space Sci. Rev.*, *70*, 215–220.

Bothmer, V., and R. Schwenn (1998), The structure of magnetic clouds in the solar wind, *Ann. Geophys.*, *16*, 1–24.

Burlaga, L. F. (1988), Magnetic clouds: Constant alpha force-free configurations, *J. Geophys. Res.*, *93*, 7217–7224.

Burlaga, L. F. (1995), *Interplanetary Magnetohydrodynamics*, pp. 89–114, Oxford Univ. Press, New York.

Burlaga, L. F., E. C. Sittler, F. Mariani Jr., and R. Schwenn (1981), Magnetic loop behind an inter-planetary shock: Voyager, Helios, and IMP-8 observations, *J. Geophys. Res.*, *86*, 6673–6684.

Burlaga, L. F., R. P. Lepping, and J. A. Jones (1990), Global configuration of a magnetic cloud, *Physics of Magnetic Flux Ropes*, *Geophys. Monogr. Ser.*, vol. 58, edited by C. T. Russell, E. R. Priest, and L. C. Lee, pp. 373–377, AGU, Washington, D. C.

Goldstein, H. (1983), On the field configuration in magnetic clouds, *Solar Wind Five*, edited by M. Neugebauer, NASA Conf. Publ., 2280, pp. 731–733.

Gopalswamy, N., et al. (1998), On the relationship between coronal mass ejections and magnetic clouds, *Geophys. Res. Lett.*, *25*, 2485–2488.

Gosling, J. T. (1990), Coronal mass ejections and magnetic flux ropes in interplanetary space, *Physics of Magnetic Flux Ropes*, *Geophys. Monogr. Ser.*, vol. 58, edited by C. T. Russell, E. R. Priest, and L. C. Lee, pp. 343–364, AGU, Washington, D. C.

Gosling, J. T. (1997), Coronal mass ejections: An overview, *Coronal Mass Ejections*, edited by N. Crooker et al., GM 99, pp. 9–16, AGU, Washington, D. C.

Leamon, R. J., C. W. Smith, and N. F. Ness (1998), Characteristics of magnetic fluctuations within coronal mass ejections: The January 1997 event, *Geophys. Res. Lett.*, *25*, 2505–2509.

Lepping, R. P., and D. Berdichevsky (2000), Interplanetary magnetic clouds: Sources, properties, modeling, and geomagnetic relationship, in

Recent Research Developments in Geophysical Research, 3, Research Signpost, pp. 77–96.

Lepping, R. P., J. A. Jones, and L. F. Burlaga (1990), Magnetic field structure of interplanetary magnetic clouds at 1 AU, *J. Geophys. Res.*, *95*, 11,957–11,965.

Lepping, R. P., et al. (1995), The WIND magnetic field investigation, The Global Geospace Mission, *Space Sci. Rev.*, *71*, 207–229.

Lepping, R. P., D. B. Berdichevsky, A. Szabo, C. Arqueros, and A. J. Lazarus (2003), Profile of a generic magnetic cloud at 1 AU for the quiet solar phase: WIND observations, *Solar Phys.*, *212*, 425–444.

Lepping, R. P., D. B. Berdichevsky, C.-C. Wu, A. Szabo, T. Narock, F. Mariani, A. J. Lazarus, and A. J. Quivers (2006), A summary of wind magnetic clouds for the years 1995–2003: Model fitted parameters, associated errors, and classifications, *Ann. Geophys.*, *24*, 215–245, SrefID: 1432-0576/ag/2006-24-215.

Lundquist, S. (1950), Magnetohydrostatic fields, *Ark. Fys.*, *2*, 361.

Marubashi, K. (1986), Structure of the interplanetary magnetic clouds and their solar origins, *Adv. Space Res.*, *6*(6), 335–338.

Marubashi, K. (1997), Interplanetary magnetic flux ropes and solar filaments, *Coronal Mass Ejections*, edited by N. Crooker et al., *Geophys. Monog.* 99, pp. 147–156, AGU, Washington, D. C.

Matthaeus, W. H., M. L. Goldstein, and D. A. Roberts (1990), Evidence for the presence of quasi two-dimensional nearly incompressible fluctuations in the solar wind, *J. Geophys. Res.*, *95*, 20,673–20,683.

Osherovich, V. I., C. J. Farrugia, and L. F. Burlaga (1993), Dynamics of aging magnetic clouds, *Adv. Space Res.*, *13*(6), 57–62.

Priest, E. (1990), *The Equilibrium of Magnetic Flux Ropes (Tutorial Lecture)*, edited by C. T. Russell, E. R. Priest, and L. C. Lee, *Geophys. Monog.* 58, pp. 1–22, AGU, Washington, D. C.

Webb, D. F., et al. (2000), The origin and development of the May 1997 magnetic cloud, *J. Geophys. Res.*, *105*(A12), 27,251–27,259.

Zank, G. P., and W. H. Matthaeus (1992), The equations of reduced magnetohydrodynamics, *J. Plasma Phys.*, *48*, 85–100.

R. P. Lepping, Space Weather Laboratory, GSFC/NASA, Greenbelt, MD 20771, USA.

T. W. Narock, Goddard Earth and Science Technology Center, University of Maryland, Baltimore County, Baltimore, MD, USA. (tom.narock@gsfc.nasa.gov)